

Dynamical Classicalization

N. Tetradis

University of Athens

- In certain nonrenormalizable field theories scattering can take place **at a length scale r_*** much larger than the **typical scale L_* of the nonrenormalizable terms** in the Lagrangian.
(Dvali, Gludice, Gomez, Kehagias, Pirtskhalava, Grojean...)
- Similar to ultra-Planckian scattering in gravitational theories, with a black hole forming at distances comparable to the Schwarzschild radius.
- The Schwarzschild radius can be much larger than the Planck length. If the formation and evaporation of a black hole are viewed as a scattering process, the cross section is determined by the Schwarzschild radius and not the Planck scale.
- In the classicalization scenario, the center-of-mass energy can be used to define the analogue of the Schwarzschild radius: **classicalization radius r_*** .
- If all scattering takes place at $r_* \gg L_*$, the fundamental scale L_* is irrelevant and no UV completion of the theory is needed.
- **Study an idealized scattering process** (Dvali, Pirtskhalava).

Outline

- Models: quartic, DBI
- Numerical method and results
- Conclusions
- Toy model
- N. Brouzakis, J. Rizos, N. T.
arXiv:1112.5546 [hep-th], to appear in JHEP
J. Rizos, N.T.
arXiv:1109.6174 [hep-th] , Phys.Lett. B 708:170 (2012)

Quartic model

- **Lagrangian density** ($\delta_1 = \pm 1$)

$$\mathcal{L} = \frac{1}{2} (\partial_\mu \phi)^2 - \delta_1 \frac{L_*^4}{4} \left((\partial_\mu \phi)^2 \right)^2.$$

- **Equation of motion**

$$\partial^\mu \left[\partial_\mu \phi \left(1 - \delta_1 L_*^4 (\partial_\nu \phi)^2 \right) \right] = 0.$$

- Idealized scattering process: **collapsing spherical wavepacket**

$$\phi_0(t, r) = \frac{A}{r} \exp \left[-\frac{(r+t-r_0)^2}{a^2} \right].$$

- Perturbation theory (Dvali, Pirtskhalava): strong deformation at the **classicalization radius**

$$r_* \sim L_* (A^2 L_* / a)^{1/3}.$$

- We have $r_* \gg L_*$ when the center-of-mass energy $s \sim A^2/a$ is much larger than $1/L_*$.

Alternative point of view (Brouzakis, Rizos, N.T.)

- With spherical symmetry, the equation of motion is ($\lambda = \delta_1 L_*^4$)

$$\begin{aligned} (1 - 3\lambda\phi_t^2 + \lambda\phi_r^2) \phi_{tt} - (1 - \lambda\phi_t^2 + 3\lambda\phi_r^2) \phi_{rr} + 4\lambda\phi_r\phi_t \phi_{tr} \\ = \frac{2\phi_r}{r} (1 - \lambda\phi_t^2 + \lambda\phi_r^2). \end{aligned}$$

- This is a **quasilinear second-order partial differential equation**

$$\mathcal{A}(\phi_t, \phi_r) \phi_{tt} + \mathcal{B}(\phi_t, \phi_r) \phi_{tr} + \mathcal{C}(\phi_t, \phi_r) \phi_{rr} = \mathcal{D}(\phi_t, \phi_r, r),$$

with **discriminant**

$$\Delta = \frac{1}{4}(\mathcal{B}^2 - 4\mathcal{A}\mathcal{C}) = 3 \left(\frac{1}{3} - \lambda\phi_t^2 + \lambda\phi_r^2 \right) (1 - \lambda\phi_t^2 + \lambda\phi_r^2).$$

- $\Delta > 0$: hyperbolic, $\Delta = 0$: parabolic, $\Delta < 0$: elliptic.
- Hyperbolic equations admit wave-like solutions, while elliptic ones do not support propagating solutions.
- If \mathcal{A} , \mathcal{B} , \mathcal{C} are evaluated for the unperturbed configuration, the discriminant switches sign in the vicinity of the classicalization radius. The equation is of **mixed type**.

- The equation of motion is equivalent to the conservation of the energy-momentum tensor

$$\partial_t \left[\frac{1}{2} (\phi_t^2 + \phi_r^2) + \frac{\lambda}{4} (-3\phi_t^4 + \phi_r^4 + 2\phi_t^2\phi_r^2) \right] - \frac{1}{r^2} \partial_r [r^2 \phi_t \phi_r (1 - \lambda\phi_t^2 + \lambda\phi_r^2)] = 0.$$

- The local energy density is

$$\rho = \frac{1}{2} (\phi_t^2 + \phi_r^2) + \frac{\lambda}{4} (-3\phi_t^4 + \phi_r^4 + 2\phi_t^2\phi_r^2).$$

- **The total energy is conserved during the evolution.**

Exact analytical solutions

- For $\phi = \phi(r)$ we obtain the **static classicalons**

$$\phi_r(1 + \lambda\phi_r^2) = \frac{c}{r^2}.$$

For a localized configuration of finite energy, $\phi_r \sim c/r^2$ for large r . This solution extends down to $r = 0$ for $\lambda > 0$, while it displays a square-root singularity at $r_s \neq 0$ for $\lambda < 0$.

- It is possible to join smoothly two singular solutions. The field ϕ would be double-valued for $r > r_s$, while it would not be defined for $r < r_s$.
- Exact **dynamical solutions** $\phi = \phi(z)$, with $z = r^2 - (t - t_0)^2$ and $h(z)$ given by the roots of the cubic equation

$$4\lambda z^2 h^3(z) + z^2 h(z) + c = 0.$$

- Square root singularities: shock waves ? (Heisenberg)

DBI model

- Lagrangian density ($\delta_2 = \pm 1$)

$$\mathcal{L} = -\frac{1}{\delta_2 L_*^4} \sqrt{1 - \delta_2 L_*^4 (\partial_\mu \phi)^2},$$

- Equation of motion

$$\partial^\mu \left[\partial_\mu \phi / \sqrt{1 - \delta_2 L_*^4 (\partial_\nu \phi)^2} \right] = 0.$$

- With spherical symmetry, the equation of motion is ($\lambda = \delta_2 L_*^4$)

$$(1 + \lambda \phi_r^2) \phi_{tt} - (1 - \lambda \phi_t^2) \phi_{rr} - 2\lambda \phi_r \phi_t \phi_{tr} = \frac{2\phi_r}{r} (1 - \lambda \phi_t^2 + \lambda \phi_r^2).$$

- **Discriminant:** $\Delta = \frac{1}{4}(B^2 - 4AC) = 1 - \lambda \phi_t^2 + \lambda \phi_r^2 \geq 0$.
- Local energy density

$$\rho = \frac{1 + \lambda \phi_r^2}{\lambda \sqrt{1 - \lambda \phi_t^2 + \lambda \phi_r^2}} - \frac{1}{\lambda}.$$

Exact analytical solutions

- **Static classicalons** ($c > 0$)

$$\phi_r = \pm \frac{c}{\sqrt{r^4 - \lambda c^2}}.$$

Field configuration induced by a δ -function source resulting from the large concentration of energy within a small region of space around $r = 0$ (Dvali, Giudice, Gomez, Kehagias).

- For $\lambda < 0$ the solutions for both signs extend down to $r = 0$. For $\lambda > 0$ they display a square-root singularity at $r_s = \lambda^{1/4} c^{1/2}$. They can be joined smoothly in a continuous double-valued function of r for $r \geq r_s$.
- A similar construction: Blons, that describe Dirichlet $(d - 1)$ -branes embedded in $(d + 1)$ -dimensional Minkowski space, with the field ϕ the transverse coordinate (Gibbons).

- Exact **dynamical solutions** $\phi = \phi(z)$, with $z = r^2 - (t - t_0)^2$ and

$$h(z) = \pm \frac{1}{\sqrt{cz^4 - 4\lambda z}}.$$

- For both signs of λ , the solutions display square-root singularities at the value $z_s = r_s^2 - (t_s - t_0)^2$ that satisfies $z_s^3 = 4\lambda/c$ ($c > 0$).
- The shock waves we encounter in the numerical solutions can be fitted by functions with square-root singularities, but with coefficients that do not match the ones deduced from the above equation.

Numerical method

- Variant of the **leap-frog scheme**.
- Discretized version of the equation of motion ($U = \phi_t$, $V = \phi_r$)

$$\begin{aligned} \frac{\Delta r}{\Delta t} r_i^2 \left[G(U_i^{j+1}, V_i^{j+1}) - G(U_i^{j-1}, V_i^{j-1}) \right] \\ = r_{i+1}^2 F(U_{i+1}^j, V_{i+1}^j) - r_{i-1}^2 F(U_{i-1}^j, V_{i-1}^j). \end{aligned}$$

- Quartic: $F = U(1 - \lambda U^2 + \lambda V^2)$, $G = V(1 - \lambda U^2 + \lambda V^2)$
- DBI: $F = U/(1 - \lambda U^2 + \lambda V^2)^{1/2}$, $G = V/(1 - \lambda U^2 + \lambda V^2)^{1/2}$
- Discretized version of the condition $\partial\phi_t/\partial r = \partial\phi_r/\partial t$

$$U_{i+1}^j - U_{i-1}^j = \frac{\Delta r}{\Delta t} (V_i^{j+1} - V_i^{j-1}).$$

Possible problems

- At some stage the solution develops a **shock front**. From this point on, the numerical integration cannot be continued, as the evolution of the shock depends on additional physical assumptions about its nature (discontinuities in the field configuration, or its derivatives).
- At some time **a real solution ceases to exist** within a certain range of r . This possibility is already apparent in the analytical solutions.
- **The equation of motion switches type** within a range of r . When it becomes elliptic, its solution requires (Dirichlet or Neumann) boundary conditions on a closed contour. The scattering problem that we are considering cannot provide such conditions, as it is set up through Cauchy boundary conditions at the initial time. Boundary conditions on a closed contour would require the values of ϕ or its derivatives at times later than the time of interest.

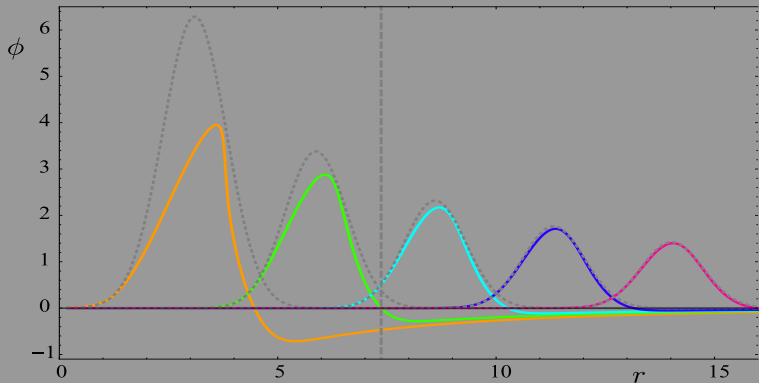


Figure: The nonlinear wavepacket at various times (solid lines) vs. the linear wavepacket (dotted lines), in the context of the **DBI model with $\delta_2 = 1$, $L_* = 1$** . The initial wavepacket has $A = 20$, $a = 1$. The vertical dashed line denotes the classicalization radius.

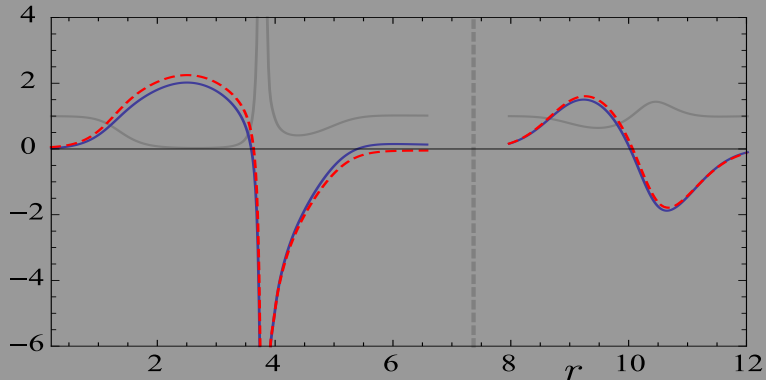


Figure: The derivatives ϕ_t (dashed) and ϕ_r (solid) of the nonlinear field, and the discriminant Δ (solid grey), at two different times, before and after the crossing of the classicalization radius. The model is the **DBI model with $\delta_2 = 1$, $L_* = 1$** . The vertical dashed line denotes the classicalization radius.

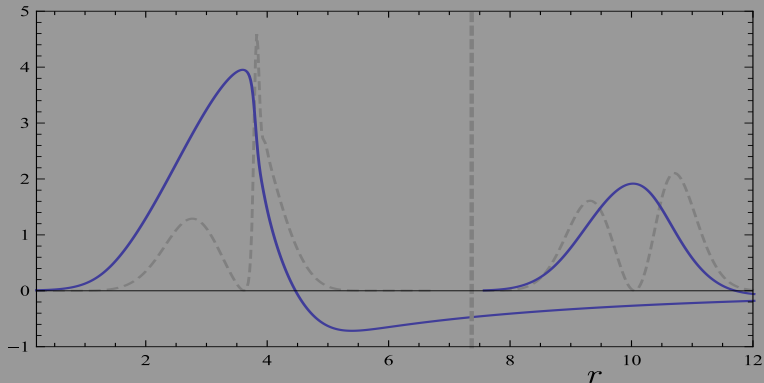


Figure: The nonlinear field ϕ (solid) and the product $4\pi r^2 \rho$, with ρ the energy density (dashed). The model is the **DBI model with $\delta_2 = 1$, $L_* = 1$** . The vertical dashed line denotes the classicalization radius. The energy density is multiplied by 5×10^{-4} .

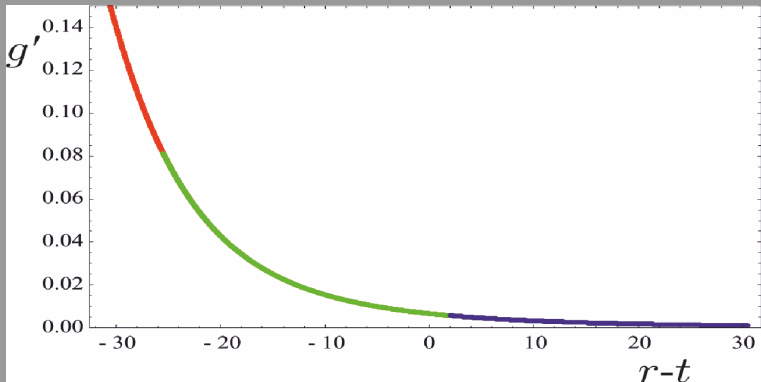


Figure: The derivative of the function $g(r - t)$ appearing in the asymptotic form $\phi(t, r) = g(r - t)/r$. A good fit can be obtained with two terms of the form $A/(r - t + c)^n$, with $n \sim 3 - 5$. The model is the **DBI model with $\delta_2 = 1$, $L_* = 1$.**

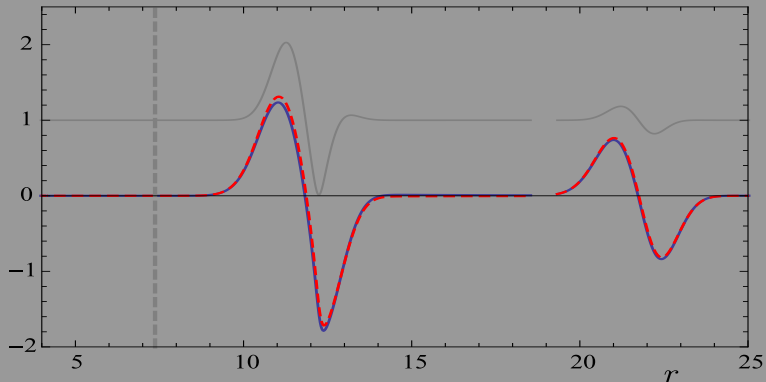


Figure: The derivatives ϕ_t (dashed) and ϕ_r (solid) of the nonlinear field, and the discriminant Δ (solid grey), at two different times, in the context of the **quartic model with $\delta_1 = -1$, $L_* = 1$** . The initial wavepacket has $A = 20$, $a = 1$. The vertical dashed line denotes the classicalization radius.

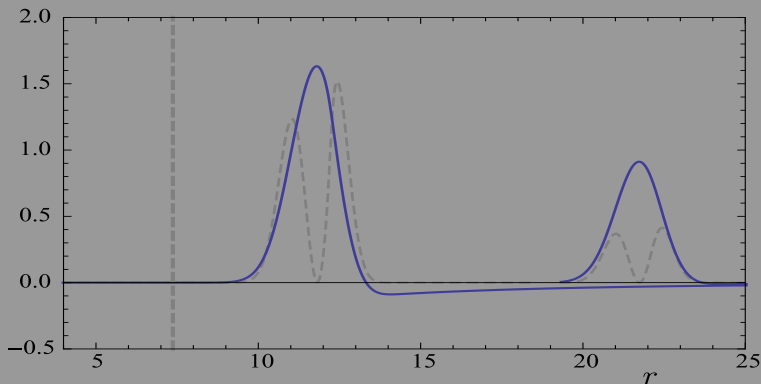


Figure: The nonlinear field ϕ (solid) and the product $4\pi r^2 \rho$, with ρ the energy density (dashed). The model is the **quartic model with $\delta_1 = -1, L_* = 1$** . The vertical dashed line denotes the classicalization radius. The energy density is multiplied by 5×10^{-4} .

Confirmed features

- The classicalization radius sets the scale for the onset of significant deformations of a collapsing classical configuration with large energy concentration in a central region.
- The equation of motion is a quasilinear partial differential equation of hyperbolic type at early times. At distances comparable to the classicalization radius, the nonlinearities become significant and can change the equation type. It seems likely that the initial conditions of the scattering process are not appropriate for the solution of the mixed type equation.
- Shock fronts develop during the scattering process at distances comparable to the classicalization radius.
- The most important observable feature of the classicalization process is the creation of an outgoing field configuration that extends far beyond the classicalization radius. This feature develops before the deformed wavepacket reaches distances of the order of the fundamental scale L_* .

Open issues

- Within the DBI model **the collapsing wavepacket can approach distances $\sim L_*$** before strong scattering appears. However, this could be a special feature of the DBI model.
- **The scattering in the early stages of the classicalization process seems to be minimal.** The tail of the field configuration carries a negligible amount of energy, because the corresponding modes are extremely soft. Within the DBI model, the bulk of the energy can end up within a region of size $\sim L_*$.
- Our analysis does not provide evidence for the creation and subsequent decay of a quasistatic classicalon configuration. Instead, **the classicalization scenario seems to be a fully dynamical process.**
- **The scattering problem may not have real solutions over the whole space.** Static classicalons seems to exist in the two cases (quartic model with $\lambda > 0$ and DBI model with $\lambda < 0$) in which a dynamical solution ceases to exist at an early stage of the evolution.

Toy quantum-mechanical model

- Analogue of the DBI model ($\delta = \pm 1$ and $\xi > 0$)

$$L = -\frac{1}{\delta \xi} \sqrt{1 - \delta \xi \dot{x}^2} - \frac{1}{2} \omega^2 x^2$$

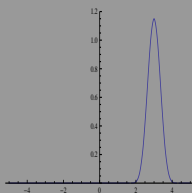
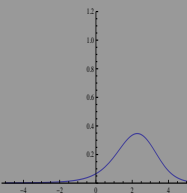
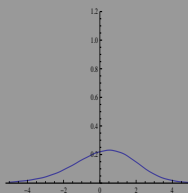
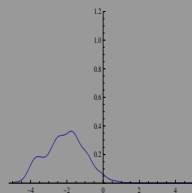
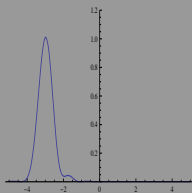
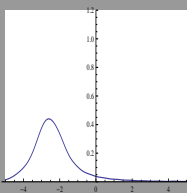
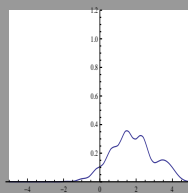
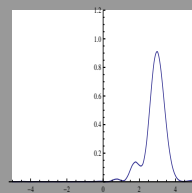
- Equation of motion: $\ddot{x} + (1 - \delta \xi \dot{x}^2)^{3/2} \omega^2 x = 0$.
- Conserved energy: $E = \frac{1}{\delta \xi \sqrt{1 - \delta \xi \dot{x}^2}} + \frac{1}{2} \omega^2 x^2 = \frac{1}{\delta \xi} + \frac{1}{2} \omega^2 x_0^2$
- $\delta = 1$: Relativistic oscillator. Analogous to DBI model with $\lambda > 0$.
- $\delta = -1$:
For $x_0^2 < 2(\xi \omega^2)^{-1}$ a real oscillating solution exists.
For $x_0^2 > 2(\xi \omega^2)^{-1}$ no real solution below $x^2 = x_0^2 - 2(\xi \omega^2)^{-1}$, where \dot{x} diverges. **Energy cannot be conserved.**
- Analogous to DBI model with $\lambda < 0$. The partial derivative with respect to ϕ_t of the energy density vanishes when $1 + \lambda \phi_r^2$ (the coefficient of ϕ_{tt} in the equation of motion) becomes zero.
- **New scale:** $\tilde{r}_* \sim L_* (A^2 L_* / a)^{1/2} > r_* \sim L_* (A^2 L_* / a)^{1/3}$.

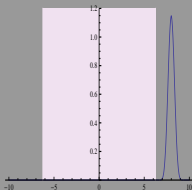
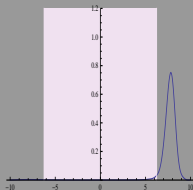
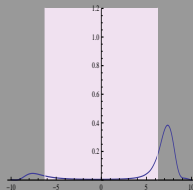
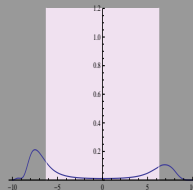
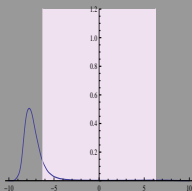
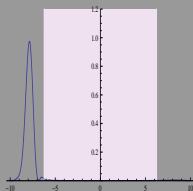
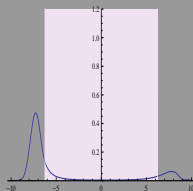
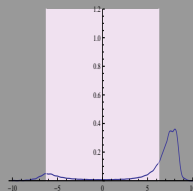
- Toy model ($\delta = -1$):
Conjugate momentum: $p = \dot{x}/\sqrt{1 + \xi\dot{x}^2}$.
It has a maximum, equal to $1/\sqrt{\xi}$, obtained for $\dot{x} \rightarrow \infty$.
- DBI model with $\lambda < 0$:
Conjugate momentum density: $\pi = \phi_t/\sqrt{1 - \lambda\phi_t^2 + \lambda\phi_r^2}$.
Its partial derivative with respect to ϕ_t vanishes at \tilde{r}_* .
- Toy model Hamiltonian: $H = \frac{1}{\xi} - \frac{1}{\xi}\sqrt{1 - \xi p^2} + \frac{1}{2}\omega^2 x^2$.
- Solve the Schrödinger equation in momentum space with

$$\hat{H} = 1 - \sqrt{1 - p^2} - \frac{1}{2}\omega^2 \frac{d^2}{dp^2},$$

requiring that the wavefunction $\psi(p)$ vanishes outside the interval $[-1/\sqrt{\xi}, 1/\sqrt{\xi}]$.

- **Construct localized wavepackets and study their evolution in x-space.**

Figure: $t = 0$ Figure: $t = 0.75$ Figure: $t = 1.38$ Figure: $t = 2.14$ Figure: $t = 2.76$ Figure: $t = 3.52$ Figure: $t = 4.90$ Figure: $t = 5.53$

Figure: $t = 0$ Figure: $t = 0.25$ Figure: $t = 0.50$ Figure: $t = 0.75$ Figure: $t = 1.01$ Figure: $t = 1.51$ Figure: $t = 1.89$ Figure: $t = 2.26$